Int. J. of Applied Mechanics and Engineering, 2017, vol.22, No.3, pp.739-747

DOI: 10.1515/ijame-2017-0046

Brief note

MODELING OF TWO-WHEELED SELF-BALANCING ROBOT DRIVEN BY DC GEARMOTORS

P. FRANKOVSKÝ, L. DOMINIK, A. GMITERKO, I. VIRGALA

Department of Mechatronics, Faculty of Mechanical Engineering
Technical University of Košice
Park Komenského 8, 042 00 Košice, SLOVAKIA
E-mail: lukas.dominik@tuke.sk

P. KURYLO*

University of Zielona Góra, Faculty of Mechanical Engineering Institute of Machine Building and Operation Zielona Góra, POLAND

O. PERMINOVA

Kalashnikov Izhevsk State Technical University 7 Studencheskaya St., 426069 Izhevsk, RUSSIA

This paper is aimed at modelling a two-wheeled self-balancing robot driven by the geared DC motors. A mathematical model consists of two main parts, the model of robot's mechanical structure and the model of the actuator. Linearized equations of motion are derived and the overall model of the two-wheeled self-balancing robot is represented in state-space realization for the purpose of state feedback controller design.

Key words: self-balancing robot, inverted pendulum, DC gearmotor, state space model.

1. Introduction

The two-wheeled self-balancing robot represents a robotic platform with two independently actuated wheels and center of gravity above the axis of the wheels rotation. The behavior of the robot is similar to the classical mechanical system of an inverted pendulum. It is an interesting system to control since it is inherently unstable and non-linear [1, 2, 3].

Such robots have made a rapid advancement over the last decade and appeared in many areas of people's daily life. The best known examples of this robotic platform are modern vehicles such as Segway or Hoverboard. Also, there are a lot of concepts based on the above mentioned robotic platform which can help people in their daily life, like for example assistant robots [1], baggage transportation robots [5] or wheelchairs for handicapped people [6]. A wide application range of these robots stems from their fundamental characteristics including compact structure and good maneuverability with zero turning radius [7, 8].

2. System modeling

In this section, the mathematical model of the robot is derived.

2.1. Mechanical subsystem

A mechanical subsystem consists of robot's body and two wheels. The body can be modelled as an inverted pendulum with the mass concentrated in the centre of gravity and the axis of rotation above the axis

_

^{*} To whom correspondence should be addressed

of wheels. For derivation of motion equations a planar model is used where robot moves along a horizontal axis, as is shown in Fig.1. Suppose that there is no slip between the wheels and the ground. The Lagrange's second order equations are used for modelling of a mechanical subsystem [4, 9].

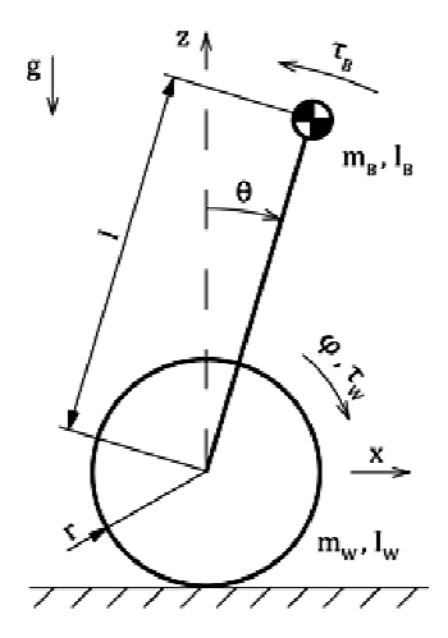


Fig.1. Free body diagram of robot's mechanical subsystem.

The no slip condition of movement is given by

$$x = r\varphi. ag{2.1}$$

The movement of robot's body COG is given by

$$x_{COG} = x + l\sin\Theta, (2.2)$$

$$z_{COG} = l\cos\Theta, \tag{2.3}$$

$$v_{COG} = \sqrt{\dot{x}_{COG}^2 + \dot{z}_{COG}^2}.$$
 (2.4)

Kinetic energy of the body is given by

$$E_{kB} = \frac{1}{2} m_b v_{COG}^2 + \frac{1}{2} I_b \dot{\Theta}^2 = \frac{1}{2} m_b \left(\dot{x}^2 + 2\dot{x}l \cos\Theta\dot{\Theta} + l^2 \dot{\Theta}^2 \right) + \frac{1}{2} I_b \dot{\Theta}^2.$$
 (2.5)

Kinetic energy of the wheel is given by

$$E_{kW} = \frac{1}{2} m_W \dot{x}^2 + \frac{1}{2} I_w \dot{\phi}^2 = \frac{1}{2} m_W \dot{x}^2 + \frac{1}{2} \frac{I_w}{r^2} \dot{x}^2.$$
 (2.6)

Potential energy of the body is given by

$$E_{pB} = m_b g l \cos \Theta. \tag{2.7}$$

Potential energy of the wheel is given by

$$E_{pW} = 0. ag{2.8}$$

We need to consider that there is also some dissipated energy as a consequence of rolling the wheels along the way. For this purpose let us write a Rayleigh dissipation function for both wheels as

$$D = 2\frac{1}{2}b_W\dot{\phi}^2 = \frac{b_W}{r^2}\dot{x}^2. \tag{2.9}$$

The Lagrangian of the system is defined as the difference between the above kinetic and potential energy

$$L = E_k - E_p = E_{kB} + 2E_{kW} - E_{pB} - 2E_{pW}. (2.10)$$

The Lagrange second order equations with the dissipation function are defined as

$$\frac{d}{dt} \left(\frac{\partial L}{\partial \dot{q}i} \right) - \frac{\partial L}{\partial qi} = Qi - \frac{\partial D}{\partial \dot{q}i}, \tag{2.11}$$

where q_i represents generalized coordinates and Q_i represents generalized forces. Generalized forces are torques from both wheels

$$Q_i = \tau_R + \tau_L. \tag{2.12}$$

Position x and angular position θ were chosen as system coordinates Substituting system coordinates into generalized coordinates we can rewrite the Lagrange second order equations and get equations of motion. For the x coordinate we obtain

$$\left(m_B + 2m_W + 2\frac{I_W}{r^2}\right)\ddot{x} + 2\frac{b_W}{r^2}\dot{x} + m_B l\cos\Theta\ddot{\Theta} - m_B l\sin\Theta\dot{\Theta}^2 = \frac{\tau_R + \tau_L}{r},$$
(2.13)

and for the θ coordinate the equation is

$$m_B l \cos \Theta \ddot{x} + \left(m_B l^2 + I_B\right) \ddot{\Theta} - m_B g l \sin \Theta = -\left(\tau_R + \tau_L\right). \tag{2.14}$$

The derived dynamic equations of motion are nonlinear. Assume that while the robot moves along the x axis only small deviations in the angular position θ are obtained. This means that we can make a linearization around an unstable equilibrium point which makes the model more suitable for controller design. Using this fact the approximations are [10, 11, 3]

$$\cos \Theta \approx I, \quad \sin \Theta \approx \Theta, \quad \dot{\Theta}^2 \approx 0,$$
 (2.15)

and linearized equations of motion are

$$\left(m_B + 2m_W + 2\frac{I_W}{r^2}\right)\ddot{x} + 2\frac{b_W}{r^2}\dot{x} + m_B l\ddot{\Theta} = \frac{\tau_R + \tau_L}{r},$$

$$m_B l\ddot{x} + \left(m_B l^2 + I_B\right)\ddot{\Theta} - m_B g l\Theta = -\left(\tau_R + \tau_L\right).$$
(2.16)

2.2. Actuator subsystem

The brushed DC gearmotors are used as the actuator subsystem of the robot [1]. The subsystem directly provides rotary motion and coupled with the wheels allows the robot to make movement. The input to this subsystem is voltage source v_s applied to the motor's armature, while the output is the rotational speed $\dot{\varphi}_W$ and torque τ_W of the gearbox shaft.

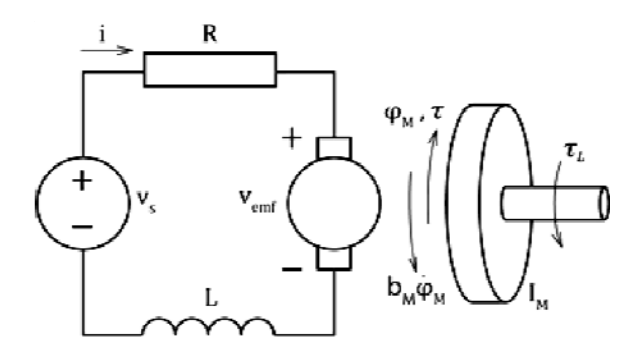


Fig.2. Electric equivalent circuit of the armature and the free-body diagram of the rotor.

The torque τ generated by a DC motor is in general proportional to the armature current i and strength of the magnetic field. Assume that the magnetic field is constant. In that case the motor torque is proportional to the armature current by constant factor k_t

$$\tau = k_t i. \tag{2.17}$$

While the shaft is rotating the back emf voltage v_{emf} is generated and is proportional to the angular velocity of the shaft by constant factor k_e

$$v_{emf} = k_e \dot{\varphi}_M. \tag{2.18}$$

The motor torque and back emf constant have the same numerical value, therefore we will use K to represent them both.

From the electrical equivalent circuit of the armature we can derive the equation

$$v_s - Ri - L\frac{di}{dt} - v_{emf} = 0. ag{2.19}$$

Given that the value of inductance L of a small DC motor is in general a very low number compared to its resistance R, we can neglect it.

From the free-body diagram of the rotor we can derive the equation

$$I_M \ddot{\varphi}_M + b_M \dot{\varphi}_M + \tau_L = \tau. \tag{2.20}$$

By putting the Eqs (2.17)-(2.20) together we obtain the equation describing the overall DC motor characteristics

$$I_M \ddot{\varphi}_M + \left(b_M + \frac{K^2}{R}\right) \dot{\varphi}_M + \tau_L = \frac{K}{R} v_s. \tag{2.21}$$

The torque τ_W required by the robot's wheel is much higher as compared to the nominal torque τ of the DC motor. In this case a gearbox needs to be applied between the motor and the wheel.

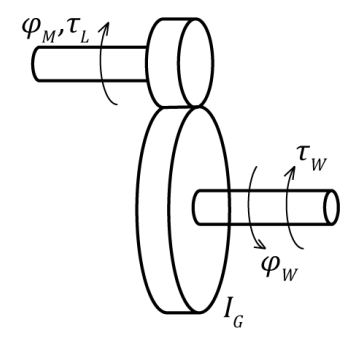


Fig.3. Free-body diagram of the gearbox.

Power exerted by the DC motor is the same at the input and at the output of the gear. It can be written as

$$\tau_L \dot{\phi}_M = \tau_W \dot{\phi}_W, \tag{2.22}$$

and then by using the gear aspect ratio n we obtain

$$\dot{\varphi}_{M} = \dot{\varphi}_{W} n,$$

$$\tau_{L} = \frac{\tau_{W}}{n}.$$
(2.23)

Substituting the above equations into Eq.(2.21) and denoting by I_G the internal inertia of the gear and by b_G the internal damping of the gear, we obtain the equation of the actuator subsystem

$$\left(I_M n^2 + I_G\right) \ddot{\varphi}_W + \left(\left(b_M + \frac{K^2}{R}\right) n^2 + b_G\right) \dot{\varphi}_W + \tau_W = \frac{Kn}{R} v_s. \tag{2.24}$$

2.3. The overall model of the robot

DC gearmotors are located between the wheels and the robot's body. As shown in Fig.1, the relation between angular coordinates is

$$\varphi - \Theta = \varphi_W. \tag{2.25}$$

Consider that both gearmotors generate similar torque, then we can write

$$\tau_R + \tau_L = 2\tau_W. \tag{2.26}$$

By substituting Eqs (2.1), (2.24), (2.25) and (2.26) into Eqs (2.16), we obtain

$$\left(\frac{m_{B}r^{2}}{2} + m_{W}r^{2} + I_{W} + I_{M}n^{2} + I_{G}\right)\ddot{\Theta} + \left(\frac{m_{B}rl}{2} - I_{M}n^{2} - I_{G}\right)\ddot{\Theta} + \left(b_{W} + b_{M}n^{2} + \frac{K^{2}n^{2}}{R} + b_{G}\right)\dot{\Phi} - \left(b_{M}n^{2} + \frac{K^{2}n^{2}}{R} + b_{G}\right)\dot{\Theta} = \frac{Kn}{R}v_{s},$$

$$\left(\frac{m_{B}rl}{2} - I_{M}n^{2} - I_{G}\right)\ddot{\Theta} + \left(\frac{m_{B}l^{2}}{2} + \frac{I_{B}}{2} + I_{M}n^{2} + I_{G}\right)\ddot{\Theta} + \left(b_{M}n^{2} + \frac{K^{2}n^{2}}{R} + b_{G}\right)\dot{\Theta} - \frac{m_{B}gl}{2}\Theta = -\frac{Kn}{R}V_{s}.$$
(2.27)

The above equations can be rewritten into a matrix form

$$\boldsymbol{E} \begin{bmatrix} \ddot{\varphi} \\ \ddot{\theta} \end{bmatrix} + \boldsymbol{F} \begin{bmatrix} \dot{\varphi} \\ \dot{\theta} \end{bmatrix} + \boldsymbol{G} \begin{bmatrix} \varphi \\ \theta \end{bmatrix} = \boldsymbol{H} \boldsymbol{v}_{s}. \tag{2.28}$$

And finally, the state space model of self-balancing two-wheeled robot is given as [12, 13]

$$\begin{vmatrix} \mathbf{\phi} \\ \dot{\mathbf{\theta}} \\ \ddot{\mathbf{\phi}} \\ \ddot{\mathbf{\theta}} \end{vmatrix} = \begin{vmatrix} 0 & 0 & 1 & 0 & 0 \\ 0 & 0 & 0 & 1 & 0 \\ -\mathbf{E}^{-1}\mathbf{G} & -\mathbf{E}^{-1}\mathbf{F} \end{vmatrix} \begin{vmatrix} \mathbf{\phi} \\ \dot{\mathbf{\phi}} \\ \dot{\mathbf{\phi}} \end{vmatrix} + \begin{vmatrix} 0 & 0 & 0 \\ \mathbf{E}^{-1}\mathbf{H} \end{vmatrix} v_{s},$$

$$\mathbf{y} = \begin{bmatrix} r & 0 & 0 & 0 & 0 \\ 0 & 1 & 0 & 0 \end{bmatrix} \begin{bmatrix} \mathbf{\phi} \\ \dot{\mathbf{\phi}} \\ \dot{\mathbf{\phi}} \\ \dot{\mathbf{\phi}} \\ \dot{\mathbf{\theta}} \end{bmatrix},$$
(2.29)

where $\varphi, \theta, \dot{\varphi}, \dot{\theta}$ are state variables. The input of the system is voltage v_s applied to the motor's armature and the outputs of the system are the tilt angle θ of the robot's body and the distance $x = r\varphi$ with which robot moves horizontally.

2.4. Robot parameters

The following table contains parameters of the modelled self-balancing robot [14, 12].

Table 1. Robot parameters.

$m_{\scriptscriptstyle B}$	Body weight	1.2 kg
$m_{\scriptscriptstyle W}$	Wheel weight	0.02 kg
$I_{\scriptscriptstyle B}$	Body inertia	0.015 kgm^2
$I_{\scriptscriptstyle W}$	Wheel inertia	0.00002 kgm^2
$I_{\scriptscriptstyle M}$	Rotor inertia	0.000001 kgm^2
I_G	Gearbox inertia	0.0001 kgm^2
$b_{\scriptscriptstyle M}$	Motor damping	0.001Nms/rad
$b_{\scriptscriptstyle W}$	Wheel damping	0.001Nms/rad
$b_{\scriptscriptstyle G}$	Gearbox damping	0.001Nms/rad
n	Gearbox ratio	30
r	Wheel diameter	0.032 m
l	COG distance	0.075 m
R	Armature resistance	2.4 Ω
K	Motor constant	0.01Nm/A

3. State-space controller

The goal is to keep a pendulum vertically while controlling the robot's movement. This problem can be solved using a state feedback controller. The schematic of this type of control is shown in Fig.4, where K is the matrix of control gains.

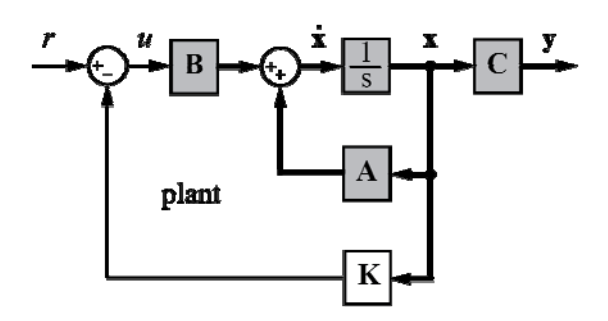


Fig.4. State feedback controller.

3.1. Controllability

Controllability can be checked by calculating the controllability matrix

$$C_o = \begin{bmatrix} B & AB & A^2B & A^3B \end{bmatrix}. \tag{3.1}$$

Considering the rank of the controllability matrix we found that the system is completely controllable from its input v_s .

3.2. Linear quadratic regulator

The linear quadratic regulator is based on minimization of a quadratic cost function

$$J = \int_{0}^{\infty} \left(\mathbf{x}^{T} \mathbf{Q} \mathbf{x} + \mathbf{u}^{T} R \mathbf{u} \right) dt , \qquad (3.2)$$

with weighting factors Q and R.

The feedback control law that minimizes the value of the cost function is given as

$$u = -Kx. ag{3.3}$$

The simplest case is to assume R = I and $\mathbf{Q} = \mathbf{C}^T \mathbf{C}$. The controller can be tuned by changing the nonzero elements in the \mathbf{Q} matrix to achieve a desirable response.

Using the state feedback controller K based on LQR design we achieve the desired behaviour of the modelled self-balancing robot. The resulting characteristic shown in Fig.5 represents the self-balancing robot exposed to the initial condition $\theta(\theta) = 0.17 rad$.

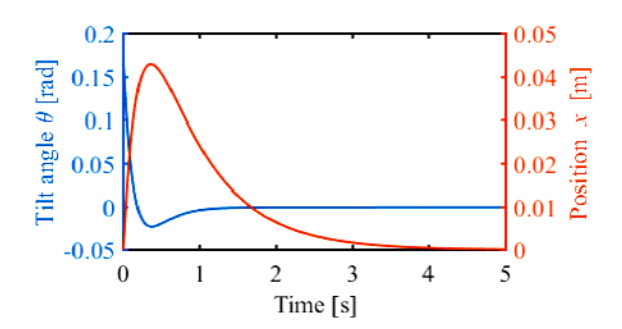


Fig.5. System response to initial condition.

The blue curve represents the robot's tilt angle in radians and the red curve represents the robot's position in meters. As you can see, the designed controller stabilizes the robot and provides the desired behaviour [3, 15].

4. Conclusions

The aim of this paper was to derive a mathematical model of a two-wheeled self-balancing robot driven by DC gearmotors. The mathematical model was successfully derived and represented in state space realization. This realization form is suitable for the purpose of the state feedback controller design to stabilize the robot about an unstable equilibrium point [10].

Acknowledgements

The authors would like to thank the Slovak Grant Agency – project VEGA 1/0872/16 and KEGA 048TUKE-4/2014.

References

- [1] Galicki M. (2016): Robust task space trajectory tracking control of robotic manipulators. International Journal of Applied Mechanics and Engineering, vol.21, No.3, pp.547-568.
- [2] Kharola A., Patil P., Raiwani S. and Rajput D. (2016): A comparison study for control and stabilisation of inverted pendulum on inclined surface using PID and fuzzy controllers. Perspectives in Science, vol.8, pp.187-190.

- [3] Chynoradský L. and Božek P. (2016): Research and development of a new system of the autonomous control of robot trajectory. Acta Mechatronica, vol.1, pp.25-28.
- [4] Jeong S. and Takahashi T. (2008): Wheeled inverted pendulum type assistant robot: design concept and mobile control. Intelligent Service Robotics, vol.1, No.4, pp.313-320.
- [5] Takei T., Imamura R. and Yuta S. (2009): *Baggage transportation and navigation by a wheeled inverted pendulum mobile robot.* IEEE Transactions on Industrial Electronic, vol.56, No.10, pp.3985-3994.
- [6] Shino M., Tomokuni N., Murata G. and Segawa M. (2014): Wheeled inverted pendulum type robotic wheelchair with integrated control of seat slider and rotary link between wheels for climbing stairs. Advanced Robotics and its Social Impacts, pp.121-126.
- [7] Grasser F., D'Arrigo A., Colombi S. and Rufer C. (2002): *JOE: A Mobile Inverted Pendulum*. IEEE Transaction on Industrial Electronics, vol.49, No.1, pp.107-114.
- [8] Fijałkowski B. (2016): Mechanical homogeneous continuous dynamical systems holor algebra steady-state alternating velocity analysis. International Journal of Applied Mechanics and Engineering, vol.21, No.4, pp.805-826.
- [9] Hendzel Z. and Rykala L. (2017): Modelling of dynamics of a wheeled mobile robot with mecanum wheels with the use of Lagrange equations of the second kind. International Journal of Applied Mechanics and Engineering, vol.22, No.1, pp.81-99.
- [10] Zhao J. and Ruan X. (2009): *The flexible two-wheeled self-balancing robot intelligence controlling based on Boltzmann*. Proceedings of the 2009 International Conference on Robotics and Biomimetics (ROBIO) on. IEEE, 2009., pp.2090-2095.
- [11] Lipták T., Kelemen M., Gmiterko A., Virgala I. and Hroncová D. (2016): *The control of holonomic system.* Acta Mechatronica, vol.1, No.1, pp.15-20.
- [12] Wu J., Zhang W. and Wang S. (2012): A two-wheeled self-balancing robot with the fuzzy PD control method. Mathematical Problems in Engineering, vol.2012, Article ID 469491, pp.13.
- [13] Sun F., Yu Z. and Yang H. (2014): A design for two-wheeled self-balancing robot based on Kalman filter and LQR. Mechatronics and Control (ICMC), 2014 International Conference on. IEEE, 2014. pp.612-616.
- [14] Per J., Ali P. and Olov R. (2009): *Two wheeled balancing LEGO robot.* Department of Information Technology, UPPSALA University, Sweden. http://www.it.uu.se/edu/course/homepage/styrsystem/vt09/Nyheter/Grupper/Rapport_group6.pdf [2017.05.01]
- [15] Kuryło P., Cyganiuk J., Tertel E. and Frankovský P. (2016): *Machine vision investigate the trajectory of the motion human body.* Review of the Methods, vol.1, No.2, pp.7-13.
- [16] Ali Y.S.E., Noor S.B.M., Bashi S.M. and Hassan M.K. (2003): *Microcontroller performance for DC motor speed control system.* Proceedings. National Power Engineering Conference, 2003. PECon 2003, pp.104-109. doi:10.1109/PECON.2003.1437427.
- [17] Mishra S.K. and Chandra D. (2014): Stabilization and tracking control of inverted pendulum using fractional order PID controllers. Journal of Engineering, vol.2014, Article ID 752918, pp.9.
- [18] Muskinja N. and Tovornik B. (2016): *Swinging up and stabilization of a real inverted pendulum*. IEEE Transactions on Industrial Electronics, vol.53, pp.631-639

Received: January 9, 2017 Revised: June 13, 2017